JOURNAL OF CATALYSIS 96, 552–562 (1985)

A Percolation Model of Catalyst Deactivation by Site Coverage and Pore Blockage

MUHAMMAD SAHIMI AND THEODORE T. TSOTSIS

Department of Chemical Engineering, University of Southern California, Los Angeles, California 90089-1211

Received April 8, 1985; revised July 9, 1985

The problem of catalyst deactivation by active site poisoning and pore blockage, under globally kinetic control, is analyzed. The catalyst pore space is represented by a three-dimensional network of interconnected pores. As a result, the effect of morphological properties of the catalyst pore space, i.e., its geometry (pore size distribution) and topology (connectedness), on the deactivation process is investigated, for the first time, simultaneously. The concepts of percolation theory, a modern theory of statistical physics of disordered media, are employed to show that both single-pore and bundle of parallel pore models perform rather poorly and that the interconnectivity of the pores plays a fundamental role in the overall catalytic behavior. The extension of the model to more complicated systems is also discussed. © 1985 Academic Press, Inc.

INTRODUCTION

The phenomenon of catalyst deactivation has been the subject of intensive research activity over the last 40 years (*1–11*). It is a very complex phenomenon which has so far defied fairly complete mathematical modeling. This is because in such a modeling one not only has to properly describe reaction and diffusion in a porous medium, as in any modern catalyst, but also to contend with the morphological changes of the pore structure. It is these morphological changes that have made the mathematical modeling of catalyst deactivation a difficult task.

It is, therefore, not surprising that almost all of the past modeling efforts have either utilized overly simplified models of porous media, such as a bundle of tubes or pseudohomogeneous descriptions in terms of macroscopic diffusivities and tortuosity factors. Both approaches have, however, a number of shortcomings. The models based on a bundle of tubes description of the pore space do account for an important aspect of porous catalysts, namely, its pore size distribution (geometry). They fail, however, to describe the effect of topology (connectedness) of the pore space. On the other hand, the pseudohomogeneous models bypass completely the problem of a reasonable description of the pore structure. They require, however, a priori knowledge of diffusivity, tortuosity factor, and surface area. Since these parameters depend on the history of the pore space, without accurate description of the pore structure one can only hope for empirical formulas. Moreover, the tortuosity factor is an ad hoc parameter whose purpose is to make the prediction of the empirical formulas agree with the data.

Recent studies have employed statistical representation of the pore structure (*12, 13*). However, they were unable to account for the important role of topology in determining the behavior of a catalyst undergoing deactivation, because of lack of realistic models for representing reaction and transport properties of the porous media. Such models, which are based on random network representation of the pore space (see below), were used by one of us in studies of flow problems in porous media (*14–17*). These studies have used the concepts of percolation theory, which is currently the state of the art of statistical physics of disordered media.

The purpose of this paper is to develop a percolation model of catalyst deactivation.

0021-9517/85 $3.00

We present the results of a study based on the concepts of percolation theory, which describes for the first time, the effect of the additional complexities that the topology of pore space introduces in the modeling of catalyst deactivation. For purpose of illustration, therefore, this paper deals with the phenomenon of deactivation under kinetic control. This assumption is very convenient in that it eliminates the complications arising by the diffusion process, which require more refined modeling than we would like to deal with in the present paper. In principle, one can apply the ideas and concepts of percolation theory to more realistic models, which are under diffusion control. Since the concepts of percolation theory have been used only in a limited number of problems of gas–solid noncatalytic and catalytic reactions (*18, 19*), another goal of this paper is to introduce to the reader these concepts with the hope that this will stimulate further research exploring the application of percolation theory in these areas.

THE BASIC EQUATIONS

In the study of the deactivation process discussed below a number of customary assumptions are made.

(I) A single catalyst particle in a differential conversion reactor is studied, i.e., the conditions at the catalyst–fluid interface do not change with time.

(II) The process is isothermal and the catalyst temperature remains constant.

(III) The fluid phase is at quasi-steady-state conditions.

It is also assumed that the catalytic material (metal) is uniformly distributed in the interior of each catalyst pore where initial concentration is C_t. A catalytic reaction occurs inside the pore at a rate r_0 [conc. products/(conc. sites)^m(unit time)]. At the same time, a side reaction occurs that results in the deposition of contaminant, which covers (poisons) active sites while simultaneously blocking part of the pore volume. The rate of the deactivation reaction is r_d [(conc. sites covered)/(conc. sites available)^n(unit time)]. The volume of deposit occupying a single site is, in general, a random variable. But for illustration purposes a pore average deposit volume b (volume/conc. sites) is used here. If one assumes that at time t after the start of the process the covered sites are uniformly distributed in the pore space (this is, of course, true for global kinetic control) and their concentration is equal to C_s, then the reaction rate in the pore and the rate of disappearance of active sites are given as follows.

The reaction rate in the pore r is given by

$$r = 2\pi RLr_o(C_t - C_s)^m \tag{1}$$

while for the site concentration one has

$$\frac{dC_s}{dt} = r_d(C_t - C_s)^n. \tag{2}$$

The available (not occupied by deposits) pore volume V_a is given by

$$V_a = \pi R^2 L - 2\pi RLC_s b = \pi R^2 L\left(1 - 2\frac{C_s b}{R}\right). \tag{3}$$

Here it is assumed that the pores are of cylindrical shape of radius R and length L. One can define an effective radius R_{eff} for a pore at time t such that

$$V_a = \pi R_{eff}^2 L \tag{4}$$

so that

$$R_{eff} = R\left(1 - 2\frac{C_s b}{R}\right)^{1/2}. \tag{5}$$

If one defines

$$\alpha = 2C_t b \tag{6}$$

and

$$\theta = r_d C_t^{n-1} t \tag{7}$$

one obtains

$$R_{eff} = R\left[1 - \frac{\alpha}{R} g(\theta)\right]^{1/2}, \tag{8}$$

where $g(\theta)$ is given by

$$g(\theta) = \begin{cases} 1 - [1 + (n-1)\theta]^{1/(1-n)} & n < 1,\ \theta < \dfrac{1}{1-n} \quad (9) \\ 1 - \exp(-\theta) & n = 1 \quad (10) \\ 1 - [1 + (n-1)\theta]^{1/(1-n)} & n > 1, \quad (11) \end{cases}$$

Note that if $\alpha < R$ then $R_{\text{eff}} > 0$ at all times, while for $\alpha \geq R$ one has $R_{\text{eff}} = 0$ after a finite time, i.e., the pore plugs (here the whole pore plugs and not just its pore mouth). This establishes a one-to-one correspondence between the plugging time θ_p and the initial radius of the pore, which will be plugged at that particular time. At any given time θ a single pore with initial radius R will be plugged as long as $R < R_b(\theta)$, where

$$R_b(\theta) = \alpha g(\theta). \quad (12)$$

The above analysis indicates that single-pore or bundle of parallel nonintersecting pores models predict that the catalyst pore structure will never plug as long as the average pore radius $\bar{R}$ (in the single-pore model) or the largest pore radius available $R_{\max}$ (in the parallel-bundle of pore model) exceeds α.

For this case and under the assumption of local or global kinetic control pore blockage has no effect on catalytic activity, and catalytic activity declines as a result of the coverage of catalytic active sites. The catalytic activity vanishes only when all active sites have been poisoned. On the other hand, if $\bar{R}$ or $R_{\max}$ is smaller than α, then the single-pore or bundle of parallel pore models predict a gradual catalytic activity decline up to a finite process time θ_p. Here θ_p, the plugging time, is the solution of the equation $g(\theta) = r/\alpha$, r being $\bar{R}$ or $R_{\max}$. Beyond θ_p there is a discontinuous drop of catalytic activity due to the fact that at θ_p all of the available pore volume has been blocked by deposits. The catalytic activity for these two models is given by the following equations.

Single-Pore Model

(I) $R > \alpha$. If r is reaction at time θ, then one has

$$r = r_i[1 - g(\theta)]^m \quad (13)$$

and one also has $r \to 0$ as $\theta \to \infty$ (i.e., $\theta_p = \infty$).

(II) $R < \alpha$

$$r = \begin{cases} r_i[1 - g(\theta)]^m & \theta < \theta_p \quad (14) \\ 0 & \theta > \theta_p \quad (15) \end{cases}$$

That is, θ_p is finite. Here r_i is the initial (at $\theta = 0$) reaction rate.

Bundle of Parallel Pores Model

As in the case of single-pore model we have two distinct cases.

(I) $R_{\max} > \alpha$. In this case an equation similar to (13) holds:

$$r = r_i[1 - g(\theta)]^m \quad (16)$$

and $r \to 0$ as $\theta \to \infty$, i.e., $\theta_p \to \infty$.

(II) $R_{\max} < \alpha$. If A_i is the fraction of initial surface belonging to blocked pores, that is

$$A_i = \frac{\int_0^{R_b(\theta)} 2\pi R L(R) f(R) dR}{\int_0^{R_{\max}} 2\pi R L(R) f(R) dR}, \quad (17)$$

where $f(R)$ is the pore size probability density function and L is the length of the pore; one has

$$r = r_i(1 - A_i)[1 - g(\theta)]^m \quad (18)$$

and $r \to 0$ and $\theta \to \theta_p$, where θ_p is finite.

It is clear that both models offer an oversimplified description of the deactivation process of commercial catalysts, which are characterized by complex interconnected porous structures. For example, Eq. (16) predicts that the catalytic activity will van-

ish only when all the available pores are blocked. In reality, of course, the internal catalyst pore structure becomes inaccessible to reaction and transport much earlier than predicted by (16). This discrepancy is due to the fact that the pores that have partially reacted and are not plugged yet become surrounded by plugged ones and become inaccessible. Thus, as the deactivation process proceeds larger and larger isolated islands of unplugged pores appear that no longer contribute to reaction and transport processes. For such a process one may intuitively expect that at some critical value of the fraction of unplugged pores, the pore space would consist of only isolated islands, so that there would be no sample-spanning paths of unplugged pores and the macroscopic connectivity of the pore space would be lost.

This picture of deactivation phenomena discussed so far is based on physical intuition. However, the same ideas also constitute the basis for the percolation theory of disordered systems, which was formally introduced by Broadbent and Hammersley (*20*) in 1957. Here those concepts of the theory, that are directly relevant to the present work, are briefly introduced and discussed, but first we give a brief description of the network model of porous catalysts.

Network Model of Porous Catalysts

Any porous medium, such as a catalyst particle, can in principle be mapped onto an equivalent three-dimensional network of random bonds connected to each other at sites or nodes of the network. All of the volume of the pore space can be assigned to the nodes or sites. Alternatively, they can be assigned to the bonds of a network, in which nodes or sites are merely mathematical points and play no fundamental role in the structure of the network and the transport and reaction processes therein. If needed one can also assign the volume of the pore space to both bonds and nodes. The geometrical characteristics of the porous medium can be incorporated into the structure of the network by assigning random radii and lengths to the network bonds and/or sites. These are selected from pore radius and length distributions that can, in principle, be obtained from porosimety or automated serial sectioning of the porous structure. The details of such a mapping are given by Lin and Cohen (*21*). Usually, the resulting equivalent network has a random topology, i.e., its local coordination number, which is the number of bonds connected to a site, is a chaotic and almost random variable. However, recent studies (*22*) show that as long as the average coordination number of the topologically disordered network is equal to the coordination number of a topologically regular network, transport and many other properties are, for all practical purposes, identical for the two networks. Because of this and since the generation of the topologically disordered networks are so costly, we employ a regular network in this study.

In the present paper we employ a three-dimensional simple-cubic network which has a coordination number of 6. Note that a simple-cubic structure is also a natural outcome of the discretization of the diffusion equation by means of finite-difference technique. To assess the effect of random topology (coordination number) on the results, a fraction of bonds of the network is removed at random to reduce the coordination number of the network to a preassigned average value. We use, as many others have in the past, a lognormal pore size distribution

$$f(R) = \frac{1}{R\sigma\sqrt{2\pi}} \exp\left\{-\frac{[\ln (R/\bar{R})]^2}{2\sigma^2}\right\}. \quad (19)$$

We further carried out computer simulations with different values of $\bar{R}$ and σ to check the qualitative effect of a narrow or broad pore size distribution on the results. All pores were assumed to have the same length.

Concepts from Percolation Theory

The natural language for describing the

topological effects is that of percolation theory. We outline in this section those concepts of the theory that are pertinent to the work presented below. Percolation theory has been reviewed by several authors (*23–25*). An excellent introduction to the subject can be found in the recent book of Stauffer (*26*).

Of all the bonds or sites, in any given network, it is convenient to designate a subset as *allowed* or *open* bonds or sites. The allowed bonds or sites are those remaining after others have been removed from consideration. For our purpose, disallowed bonds will be removed by setting their radii equal to zero, because they have been plugged as the result of the chemical reaction. With enough open bonds, a continuous path of connectedness, and thus transport and reaction of allowed bonds, will span the network. In Fig. 1 we present three stages of the process of removal of bonds from a square network. As the fraction X of open bonds is decreased from unity to $\frac{2}{3}$ small islands of isolated bonds appear that have no connection to the sample-spanning cluster of open (unplugged) bonds. A cluster is a set of connected open bonds. If the fraction of open bonds is further decreased to $\frac{1}{3}$, no sample-spanning cluster will exist and the network will lose its global connectivity. Percolation quantities of interest here are the following.

(1) *Accessibility,* measured by the *accessible or percolation fraction* X^A, which is the probable fraction of network bonds (or sites) in the sample-spanning cluster.

(2) *Effectiveness,* measured by the *backbone fraction* X^B, the probable fraction of bonds (or sites) active to transport, i.e., the accessible fraction minus its dead end or the singly connected bonds that do not contribute to the transport process.

(3) *Percolation threshold* X_C, the largest fraction of allowed bonds or sites, below which the accessible fraction is zero, i.e., the network loses its global connectivity. For example, if the removal of bonds of the square network of Fig. 1 is completely random, then $X_C = \frac{1}{2}$, i.e., at least 50% of the bonds of the network have to be open in order for the network to have macroscopic or global connectivity. Obviously, for $X < X_C$ all allowed or open bonds are in the isolated clusters and therefore all macroscopic transport properties of the network, such as conductivity and diffusivity, are zero.

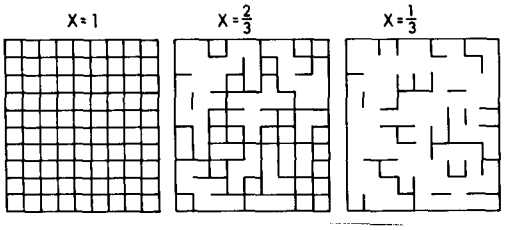

FIG. 1. Bond percolation on a square network.

The percolation model of the deactivation phenomenon presented in this paper is somewhat different from the ordinary (random) bond-percolation process described above. In the ordinary bond-percolation process, which was originally proposed by Broadbent and Hammersley, a bond is chosen at random and is designated as blocked or disallowed or closed. Thus, there is no correlation between what happens to a given bond and its neighboring bonds. In the percolation model discussed here, a bond may be blocked simply because it was originally surrounded by bonds that had smaller radii and therefore their plugging times were shorter and plugged earlier. Thus, even though a bond is still unplugged (partially reacted), it may not be reached by the reacting molecules because its nearest-neighbor bonds have already been plugged. The present percolation model is therefore a correlated one. As a result one expects to have a higher percolation threshold X_C for our model than that of the ordinary (random) bond-percolation threshold described above. Indeed, our simulations, which are described below, show that for our model $X_C \approx 0.255$ for an infinitely large simple cubic network, whereas $X_C \approx 0.249$ for the same network for the ordinary (random) bond-percolation process. Therefore, the

percolation threshold of a network is sensitive to the details of the process of removal (blockage) of the bonds.

Monte Carlo Simulations Technique

In this section, the details of the Monte Carlo simulations technique are described. Although a simple-cubic network was employed in the present study, the technique presented here is general and can be used with any network. We have first distributed the radii of the bonds of the network according to the preassigned pore size distribution. More precisely, for bond i of the network we have picked a random number ρ_i by using the random number generator of the computer, which generates random numbers that are uniformly distributed in the interval (0, 1). Then, the radius R of the pore is the solution of the equation

$$\rho_i = \int_0^R f(x)\, dx. \tag{20}$$

This procedure eliminates any need for using a discrete $f(R)$ or imposing any lower or upper bounds on the range of pore sizes, as a number of authors have done in the past.

After generating the network with the given pore size distribution the plugging times θ_p of all bonds of the network were calculated. In the present paper we used Eq. (10) but Eqs. (9) and (11) are equally easy to use and pose no special difficulty. The fully connected network with all bonds having a random nonzero radius corresponds to zero process time. Then the process time was increased sufficiently large that some pores would plug. Then a search in the network was performed in order to identify all bonds, whose plugging times were shorter than the process time. The radii of all such bonds were set to zero. We then performed another search in the network to identify all accessible bonds and those unplugged bonds, that have been surrounded by plugged ones, i.e., the isolated clusters in the language of percolation theory. The process time was then increased again but this time the search was performed only among the previously accessible bonds; the isolated clusters were left untouched. This process continues, until the network has reached its percolation threshold and lost its global connectivity, at which time the process is stopped.

Strictly speaking, the percolation theory applies to systems that are infinite in size. Infinite networks defy simulation, and thus one has to use a large enough network, so that the results are representative of much larger systems and do not depend on the network size. In order to find a reasonable network size we have used the following method. We have defined an effective percolation threshold $X_C(l)$ for a network of linear dimension l (number of sites in each direction) by taking it to be the fraction of open (unplugged) bonds, at which the accessible fraction of bonds is smaller than some arbitrary chosen small value ε (in the study $\varepsilon \approx 10^{-3}$). According to the finite-size scaling theory (*27*) one has

$$X_C(\infty) - X_C(l) = al^{-\beta}, \tag{21}$$

where $X_C(\infty)$ is the percolation threshold of the infinitely large network and a and β are constant. This equation is thought to be valid for moderate and large values of l. We have thus determined $X_C(l)$ for l = 10, 13, 16, 19, and 22 by the above Monte Carlo procedure. For each value of l we made many independent realizations of the network, i.e., we repeated the process of determining $X_C(l)$ for many different assignments of pore radii and the results were averaged over the number of realizations. For each value of l enough realizations were made so that the standard deviations of the average values were small (about 5% of the averages). The results were then fitted to Eq. (21) to find simultaneously the best values of $X_C(\infty)$, a and β. They are given by

$$X_C(\infty) = 0.255$$

$$a = 0.34$$

$$\beta = 1.15.$$

Therefore, the effective percolation threshold of a 25 × 25 × 25 simple-cubic network (i.e., $l = 25$) is estimated to be about 0.247, if the above values of a, b, and $X_C(\infty)$ are used in (21) with $l = 25$, only 3.3% smaller than $X_C(\infty)$. Thus, for reasons of economy all of our simulations were performed on a simple-cubic network with $l = 25$. We have also made 25 independent realizations of each network with distributed pore sizes and averaged the statistics of interest over these realizations. We believe the results are qualitatively representative of the process in much larger systems, and the effect of the finiteness of the network size is small. The finite-size scaling theory can be used to estimate the variations of any quantity of interest with the network size; see, e.g., Sahimi *et al.* (*28*) for details.

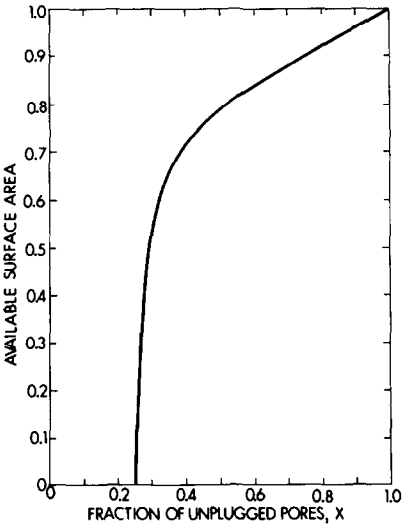

FIG. 3. Available surface area as a function of allowed fraction for the complete cubic network. $\bar{R} = 100$, $\sigma = 0.6$, $\alpha = 800$.

RESULTS AND DISCUSSIONS

The first quantity that was investigated was X^A, the accessible fraction of unplugged pores. In Fig. 2 we present X^A as a function of X, the total fraction of unplugged pores. At high values of X one has $X^A \approx X$, i.e., there is no isolated unplugged pore and all of the unblocked pores are accessible and are in the sample-spanning cluster. As X decreases (with process time) there appear isolated unplugged pores and thus the difference between X^A and X becomes significant, a feature that only percolation theory is capable of producing. In the bundle of parallel pores model one has, at all time, $X^A = X$. Below $X = 0.50$, X^A decreases sharply and as the percolation threshold X_C is approached this decrease becomes more pronounced. The accessible fraction X^A finally vanishes at $X = X_C$ and the slope of the curve at $X = X_C$ is *infinite*. The shape of this curve is qualitatively similar to those found for the ordinary (random) bond-percolation processes; see, for example, Kirkpatrick (*29*).

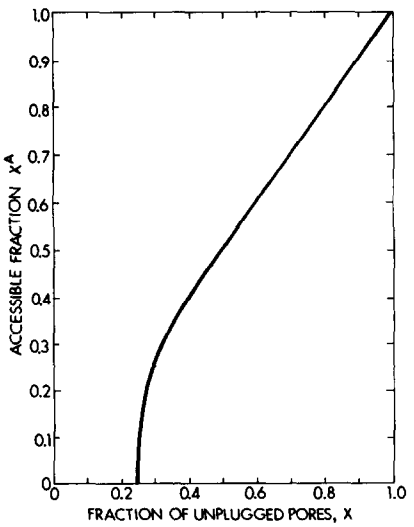

FIG. 2. Accessible fraction, X^A, as a function of allowed fraction X for bond percolation on the complete cubic network. $\bar{R} = 100$, $\sigma = 0.6$, $\alpha = 800$.

Also calculated was the available surface area of the unplugged pores, i.e., the surface area of the accessible pores. The variation of this quantity with X is displayed in Fig. 3 and as can be seen it is qualitatively similar to Fig. 2. This is expected due to the fact that the available surface area must be proportional to the accessible fraction of unplugged pores. As in Fig. 2 the available surface area sharply decreases as X_C is neared and vanishes (with infinite slope) at $X = X_C$.

Next we investigated the catalyst plug-

ging time θ_p, i.e., the time at which the catalyst becomes completely deactivated. Of course, in industrial practice the useful catalyst lifetime is usually considerably shorter than the true plugging time. However, θ_p represents the upper limit of a catalyst's useful lifetime and as such it is an important parameter of the process. In Fig. 4 we present the variation of θ_p with the average coordination number $\bar{Z}$ of the network for different values of the deposit size parameter. The reader is reminded that $\bar{Z}$ is the measure of the interconnectivity of the porous structure. Most industrial catalysts are expected to have an average coordination number between 3 and 6. As can be seen the plugging time increases as $\bar{Z}$ increases and the effect is more pronounced for smaller values of α, i.e., for small initial metal loadings C_t or small values of average molal volumes of deposits b. Such behavior is, of course, not surprising since catalysts with higher $\bar{Z}$ have on the average larger number of alternate paths for material transport than catalysts with lower $\bar{Z}$. As α increases, however, the effect of interconnectivity diminishes. For $\alpha = 1500$ the internal pore structure is destroyed at such a rapid rate, that even the presence of a highly interconnected structure has a rather insignificant effect. In all cases θ_p vanishes at $\bar{Z} \approx 1.53$, which is, of course, the mean coordination number at the percolation threshold of the simple-cubic network ($\bar{Z} \approx 0.255 \times 6 = 1.53$). This means that no macroscopically interconnected structure can exist on a simple-cubic network with a $\bar{Z}$ less than 1.53.

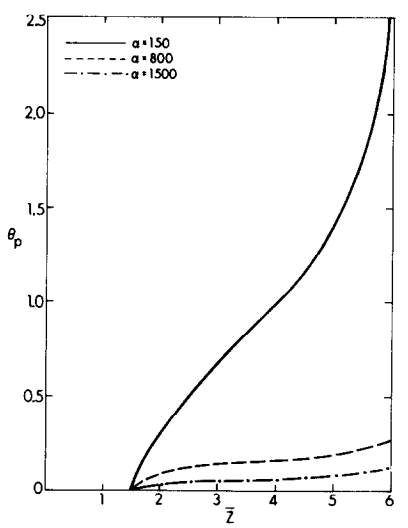

FIG. 4. Plugging time θ_p as a function of the average coordination number $\bar{Z}$ for different values of the deposit parameter α. $\bar{R} = 100$, $\sigma = 0.6$.

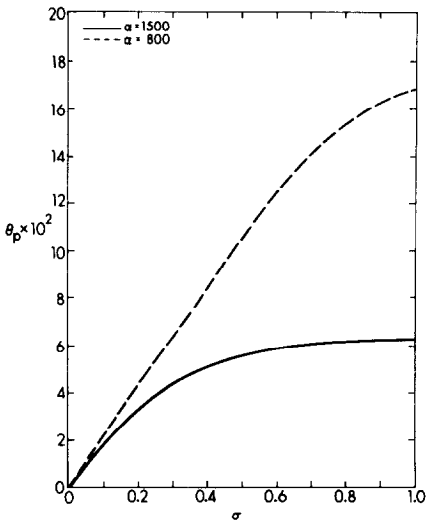

FIG. 5. Plugging time θ_p as a function of σ, for different values of the deposit parameter α. $\bar{R} = 50$, $\bar{Z} = 6$.

In Fig. 5 we present the dependence of the plugging time on σ. Large values of σ correspond, of course, to a more uniform pore size distribution, while small values of σ correspond to a narrow one centered around $\bar{R}$. Since in Fig. 5 $\bar{R}$ is smaller than α, θ_p vanishes with σ as expected. With a bundle of parallel pores model one should expect θ_p to diverge with σ. Strictly speaking, for this model θ_p should diverge as long as $\sigma \neq 0$, since there is a finite probability that a pore in this model has a radius larger than α if $\sigma \neq 0$. However, for the simple-cubic network structure used here θ_p is a slowly increasing function of σ, which is in sharp contrast with the prediction of bundle of parallel pores model.

The dependence of the normalized catalyst activity, that is, the ratio of the reaction

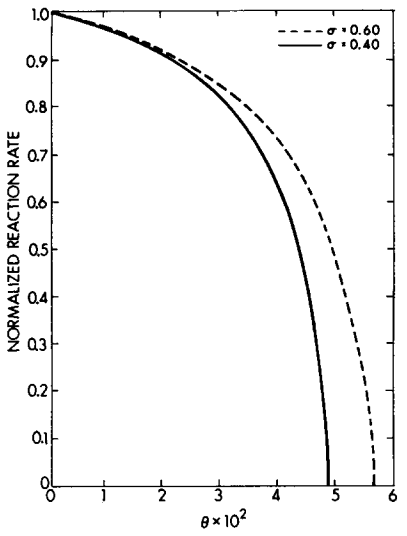

FIG. 6. Normalized reaction rate as a function of time for different values of σ. $\bar{R} = 100$, $\alpha = 1500$, $\bar{Z} = 6$.

rate at time θ to the initial reaction rate at $\theta = 0$, on the process time for two values of σ is presented in Fig. 6. As expected, the plugging time at which the catalyst activity vanishes is dependent upon σ. Figures 7 and 8 show the variation of the normalized catalyst activity on the parameter α at different process times. The qualitative

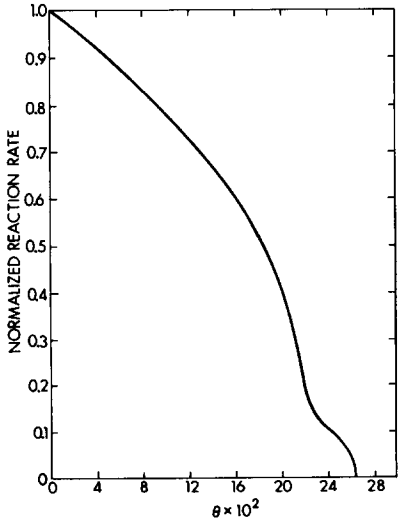

FIG. 7. Normalized reaction rate as a function of time. $\bar{R} = 100$, $\sigma = 0.6$, $\alpha = 800$, $\bar{Z} = 6$.

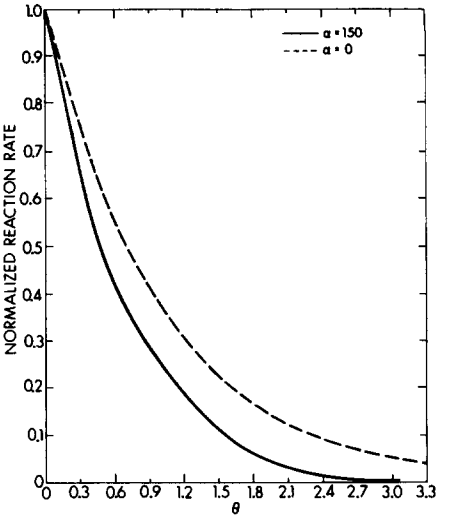

FIG. 8. Normalized reaction rate as a function of time. $\bar{R} = 100$, $\sigma = 0.6$.

changes in the shape of the activity curve with variations in α are striking. As one proceeds from Fig. 6, where pore plugging effects predominate to Fig. 8 where poisoning effects prevails, the qualitative features of activity curves change distinctly. The inflection point shown in Fig. 7 is typical of all cases characterized by intermediate values of α and qualitatively agrees with recent experimental observations with the coal liquefaction and coal–liquid hydroprocessing reaction systems (*29*). These are also characterized by two distinct regimes of rapid catalytic activity decay.

Finally, Fig. 9 displays the normalized

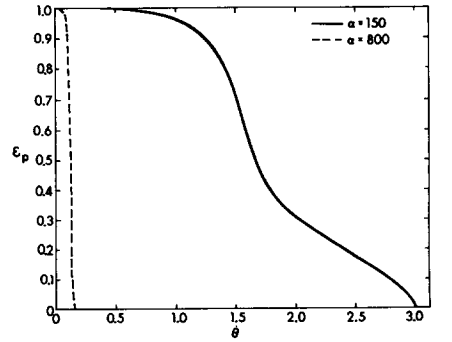

FIG. 9. Normalized porosity as a function of time for different values of deposit parameter α. $\bar{R} = 100$, $\sigma = 0.6$, $\bar{Z} = 6$.

catalyst porosity (i.e., the ratio of catalyst porosity at time θ to catalyst porosity at $\theta = 0$) as a function of time. As expected, this quantity vanishes at the percolation threshold corresponding to the plugging time.

SUMMARY AND CONCLUSIONS

We have investigated the behavior of catalytic systems undergoing deactivation by site coverage and pore blockage under global kinetic control. The catalyst pore space has been represented by a three-dimensional random network and a percolation model of catalyst deactivation process has been developed. By performing Monte Carlo simulations it has been established that the single-pore and the bundle of parallel pores models, which in the past had found an almost exclusive use in this area, perform rather poorly, qualitatively as well as quantitatively. The interconnectivity of the porous structure, expressed in terms of an average coordination number $\bar{Z}$, has been shown to play a fundamental role in the overall catalytic behavior. More interconnected porous structures have been shown to be more resistant to catalyst deactivation due to pore plugging. The qualitative shape of the activity-decline curve was shown to depend on the dimensionless parameters α, which increases as the initial metal loading (expressed in terms of C_t) or the molal volume of the deactivating deposit increases. The assumption of global kinetic control made in this paper was one of convenience rather than necessity since the main goal of this paper was to introduce to the reader the concepts of percolation theory and its associated Monte Carlo technique. By using percolation theory one may develop more elaborate models of catalyst deactivation. Work in this direction is reported elsewhere (*30*).

APPENDIX: NOMENCLATURE

A_i fraction of initial surface area belonging to blocked pores
a parameter defined in Eq. (21)
b deposit molal volume
C_s concentration of sites covered by deposits
C_t total concentration of sites
l linear dimension of the network, i.e., number of sites in each direction
L pore length
m coefficient in rate r_0
n coefficient in rate r_d
R radius of pore
$\bar{R}$ median radius for pore size distribution, Eq. (19)
r reaction rate in a pore
r_0 main reaction rate
r_d deactivating reaction rate
R_{eff} effective radius defined by Eq. (5)
r_i initial reaction rate at $\theta = 0$
R_{max} maximum radius in the pore size distribution
X fraction of allowed bonds
X^A accessible fraction
X^B backbone fraction
X_C percolation threshold
V_a available pore volume
$\bar{Z}$ average coordination number

Greek Symbols

α dimensionless deposit volume, Eq. (6)
β parameter in Eq. (21)
θ dimensionless time, Eq. (7)
θ_p plugging time
σ shape factor for pore size distribution, Eq. (19)

REFERENCES

1. Maxted, E. B., *in* "Advances in Catalysis" (D. D. Eley, H. P. Ines, and P. B. Weisz, Eds.), Vol. 3, p. 199. Academic Press, New York, 1951.
2. Voorhies, A., *Ind. Eng. Chem.* **37,** 318 (1945).
3. Wheeler, A., *in* "Catalysis" (P. M. Emmett, Ed.), Vol. 9, p. 105. Reinhold, New York, 1955.
4. Butt, J. B., *Adv. Chem. Ser.* **109,** 259 (1972).
5. Butt, J. B., and Billimoria, R. M., *ACS Symp. Ser.* **72,** 288 (1978).
6. Butt, J. B., *in* "Catalytic Deactivation" (B. Delmont and G. F. Froment, Eds.), p. 21. Elsevier, Amsterdam, 1980.
7. Froment, G. F., *in* "Catalyst Deactivation" (B. Delmont and G. F. Froment, Eds.), p. 1. Elsevier, Amsterdam, 1980.
8. Hegedus, L. L., and McCabe, R. W., *in* "Catalyst

Deactivation" (B. Delmont and G. F. Froment, Eds.), p. 471. Elsevier, Amsterdam, 1980.
9. Froment, G. F., *in* "Proceedings, 6th International Congress on Catalysis, London, 1976" (G. C. Bond, P. B. Wells, and F. C. Tompkins, Eds.), Vol. 1, p. 10. The Chemical Society, London, 1976.
10. Tsakalis, K. S., Tsotsis, T. T., and Stiegel, G. J., *J. Catal.* **88,** 188 (1984).
11. Yortsos, Y. C., and Tsotsis, T. T., *Chem. Eng. Commun.* **30,** 311 (1984).
12. Beeckman, J. W., and Froment, G. F., *Ind. Eng. Chem. Fundam.* **21,** 243 (1982).
13. Beeckman, J. W., and Froment, G. F., *Ind. Eng. Chem. Fundam.* **18,** 3 (1979).
14. Sahimi, M., *in* "Random Walks and Their Applications to the Physical and Biological Sciences" (M. F. Shlesinger and B. J. West, Eds.), p. 189. AIP, New York, 1984.
15. Sahimi, M., Davis, H. T., and Scriven, L. E., *Chem. Eng. Commun.* **23,** 329 (1983).
16. Sahimi, M., Hughes, B. D., Scriven, L. E., and Davis, H. T., *J. Chem. Phys.* **78,** 6849 (1983).
17. Heiba, A. A., Sahimi, M., Scriven, L. E., and Davis, H. T., *SPE J.*, in press.
18. Mohanty, K. K., Ottino, J. M., and Davis, H. T., *Chem. Eng. Sci.* **37,** 905 (1982).
19. Yortsos, Y. C., and Sharma, M., submitted for publication.
20. Broadbent, S. R., and Hammersley, J. M., *Proc. Cambridge Philos. Soc.* **53,** 629 (1957).
21. Lin, C., and Cohen, M. H., *J. Appl. Phys.* **53,** 4152 (1982).
22. Jerauld, G. R., Scriven, L. E., and Davis, H. T., *J. Phys. C* **17,** 3429 (1984).
23. Stauffer, D., *Phys. Rep.* **54,** 1 (1979).
24. Essam, J. W., *Rep. Prog. Phys.* **43,** 833 (1980).
25. Sahimi, M., *Lect. Notes Math.* **1035,** 314 (1983).
26. Stauffer, D., "Introduction to Percolation Theory." Taylor & Francis, London, 1985.
27. Fisher, M. E., *in* "Critical Phenomena" (M. S. Green, Ed.), Enrico Fermi Summer School, 1971 Course, p. 1. Academic Press, New York, 1971.
28. Sahimi, M., Hughes, B. D., Scriven, L. E., and Davis, H. T., *J. Phys. C* **16,** L521 (1983).
29. Steigel, J., Tischer, R. F., and Narain, N. K., PETC Quarterly Progress Report, DOE DE89004609, 1983.
30. Sahimi, M., submitted for publication.